RECONSTRUCTION OF MULTI-SCALE HETEROGENEOUS POROUS MEDIA AND THEIR FLOW PREDICTION

K. Wu, Z. Jiang, G. D. Couples, M.I.J. Van Dijke, K.S. Sorbie
Institute of Petroleum Engineering, Heriot-Watt University, Edinburgh UK

This paper was prepared for presentation at the International Symposium of the Society of Core Analysts held in Calgary, Canada, 10-12 September, 2007

ABSTRACT

Fluid flow in, and the thermal, electrical, and acoustic properties of porous media are determined primarily by the geometry and topology of the pore system. Here we illustrate a stochastic 3D space reconstruction model that uses thin section images as its main input. The approach involves a third-order Markov mesh that creates the reconstruction in a single scan; and overcomes the computational issues normally associated with Markov chain methods. The technique is capable of generating realistic "pore architecture models" (PAMs), and examples are presented for a range of fairly homogenous rock samples. PAMs, or tomography models, serve as input for another suite of analysis techniques that we call pore analysis tools (PATs). PATs allow us to quantify important characteristics of the pore system, such as the pore-size distribution, and the pore connectivity. Using PATs, we are able to extract well-characterized network models that can be used for simulating two- and three-phase fluid flow. The aim of this paper is to explore how we can use PAMs/PATs to gain additional understanding of the characteristics of porous media which contain multiple scales of pores. When such materials possess pore systems that have an extreme range of pore sizes, we are able to overcome (to some extent) the difficulties of the multiple scales by creating and analysing multiple reconstructions based on different-resolution input images.

1. INTRODUCTION

Quantitative characterisation of porous media at the pore scale is of fundamental importance in many scientific subjects. The pore structure of reservoir rocks is complex, but the geometry and topology of porous rocks must be known if we wish to *a priori* predict physical rock properties. The pore geometry ultimately affects many macroscopic phenomena associated with mechanical, acoustic and fluid flow properties.

Previous attempts to quantitatively characterise the microstructure adopt the conventional paradigm of "pore bodies" linked by smaller connections or "pore throats". In realistic porous media, fluid flow at the pore scale occurs within a complex three-dimensional (3D) network of pores. Typically, the pore network is an interconnected three-dimensional array of void spaces (e.g. in rocks, inter-granular porosity, fracture apertures, moldic porosity, etc) that can be characterised by geometrical quantities (pore size or volume, pore shape)

and topological descriptors (pore connectivity). Progress in studying transport through heterogeneous porous media has been hampered by the difficulties involved in characterizing the complex microstructure of the pore system of real materials. There is a lack of effective and efficient methods to generate models of the complex microstructures, due to difficulties in analysing the precise geometry and topology of the pore system.

Although direct measurements of a 3D microstructure are now available via synchrotron X-ray computed microtomography (Dunsmoir *et al.*, 1991; Spanne *et al.*, 1994; Hazlett, 1995, Ans *et al*., 2001), it is often difficult and expensive to obtain reliable "images" of the 3D pore structure. Such methods are also limited in terms of their scale of resolution, and there is a trade-off between resolution and sample size, which in turn relates to sample representativity. There are several techniques have been proposed to statistically generate 3D pore structures from spatial information derived from such 2D images (Joshi, 1974; Quiblier, 1984; Roberts, 1997; Hazlett, 1997; Yeong and Torquato, 1998; Manswart and Hilfer, 1998). Recent quantitative comparisons of these models with tomographic images of sedimentary rocks have shown that statistical reconstructions may differ significantly from the original sample in their geometric connectivity (Hazlett, 1997; Biswal et al., 1999; Manswart et al., 2000). In a different approach to the stochastic generation of 3D pore structures, Bakke and Øren (1997) have developed a process-based reconstruction procedure, which directly models the particle sedimentation process and was applied to reconstruct Fontainebleau sandstone, but this method involves intensive computing. This paper outlines a new reconstruction method that belongs to the class of stochastic pore space modelling. The new method creates reconstructions of a heterogeneous (possibly) porous medium using Markov Chain Monte Carlo (MCMC) simulation. It considers spatial structure information (derived from 2D or 3D sample data – specifically, thin section data in the x, y and z planes) that identifies all the transition probabilities between the voids and solids of the medium for a given local training lattice stencil. The input data is taken from image analysis, but our approach differs in one very important respect from published two-point (or multi-point) correlation methods (e.g. Okabe and Blunt, 2004). The method that we have developed involves a multiple-voxel interaction scheme (a high-order neighborhood system) to generate individual realisations that have structure characteristics matching the input data. This MCMC reconstruction approach and the models it generates are referred to as "pore architecture models", or PAMs.

Due to the complex morphology of naturally occurring pore systems, another approach is to ignore the detailed structure of the porous medium and simply to represent the microstructure by an interconnected network based on the assumption that larger pores (pore bodies) are connected by smaller pores (throats) (Fatt, 1956; Øren and Pinczewski, 1992; Blunt et al., 1995; Mani and Mohanty, 1998; van Dijke and Sorbie 2002). The most difficult task in creating such a network is identifying and specifying the coordination number and the size distributions for pore bodies and pore throats. The second task of this work is to develop efficient and accurate algorithms for mapping the pore geometry and topology of porous media both for directly scanned images (e.g. from micro CT scans) and for simulated images, e.g. generated using pore architecture models, PAMs (Wu *et al*

2006), or other approaches. In addition to the reconstruction method to produce the PAMs, we have also developed a set of tools – referred to as "pore analysis tools" or PATs – to quantitatively analyse the geometry and topology of the pore system of the reconstructed material. In this paper, we additionally set out to: (i) develop an approach to link quantifiable measures of porous media to an accurate mapping of the pore morphology; (ii) develop a methodology for using detailed information on pore morphology as an input to an invasion percolation simulator, and to compare its results with experimental data; and (iii) investigate quantitative methods for the characterization of pore connectivity and topology.

This paper describes a new approach to make predictions of the transport characteristics of porous media that possess multiple-scales of pore systems. Our approach is to numerically reconstruct the pore space of each scale of pore system from appropriately-imaged thin section. The model at each scale can then be used to predict the flow response for that part of the medium. We illustrate the value of this scheme by calculating the mercury-injection response of a siltstone.

2. RECONSTRUCTION

The concept underpinning the PAMs method originates from image processing research, where Markov Random Fields (MRFs) are widely used (Geman and Geman, 1984). MRF theory is based on using only a small number of *local* conditions to predict global features based on training images. In other words, it considers the interaction (or dependence) of a few local neighbours, and some other geometrical descriptors, to generalise the overall morphological features of the image. In typical usage, the image is pixelated, and the probability of each pixel of the model being in a particular state (black or white, for example) is determined (or conditioned) by means of a transition matrix of conditional probabilities that is determined from the training (prior) image. The key point here is that the PAM reconstruction method is based on a small template that embodies the probabilities that are used to make the reconstruction. The multi-point statistics scheme (Okabe and Blunt 2004) also uses small templates, but in those methods, the probabilities of all possible templates must be determined, and the resulting method is computationally expensive. The details of the PAMs method are described in Wu et al (2006).

We have applied the PAMs approach to a wide range of rocks and soils, encompassing perhaps 100-150 different materials to date. Here we describe the results for a variety of rock types, ranging from coarse sandstone to a very fine mudrock (Fig. 1; Table 1), to illustrate the capability of the new modelling approach. The measured permeability of these materials ranges over more than six orders of magnitude. In this paper, the emphasis is put on multi-scale heterogeneous rock images, in which case the rock has distinctive macropores (pore size in millimetres) and micropores (pore size in micrometers or submicron) systems, such as carbonate and siltstone. We obtained thin section images under different microscope magnifications. Then, our 3D Markov random field models were used to reconstruct a representative system at each scale in 3D based on these input images.

The reconstruction proves to be relatively simple for the case of typical reservoir sandstones. The challenges arise when we consider the more difficult rocks, such as carbonates, deformed rocks, siltstone etc. The main reasons are that the pore system in these rocks has multi-scale features, e.g. macropores and micropores coexist, therefore multi scaled images have to be involved. The micro pore can be mapped in a fine scale (submicron) image, while coarse resolution images have to be used to handle the macro pore and fracture in a relatively large size frame. Because of computer memory limitations, we can only deal with small volume of 3D image (perhaps to 500^3 voxels). If the model has macropores, then in a high resolution reconstruction, there would be only a few scattered large pores which would dominate. For example in Fig 1f, the reconstructed cube is 300x300x300 in volume of voxels and the resolution is 1 voxel = 0.14 microns. If we have microspores, say at 28 micron in diameter in the cube, then the single pore will take up about 214^3 voxels -70 % of the volume of the cube. In addition, the transition probabilities, derived from the training image, would not properly represent the micropores. To overcome this problem, we sub-sample a small part of the training image at high resolution, focusing on the smaller pores, i.e. the high resolution training image does not contain any complete big (macro) pores), and we reconstruct a separate model that gives a good representation of the micropore system.

Table 1. Characteristics of reconstructions and simulated permeabilities

Sample	Type	Image size (mm^2) and pixel size (μm)	Porosity (%)	Measured permeability (mD)	Simulated permeability (mD)
a	Sandstone	3.0 x 1.9 4.0	27.17	2500	2236
b	Deformed rock	1.30 x 0.92 1.0	18	82.1	71.5
c	Sandstone with sheer band	3.0 x 1.9 4.0	21.8	NA	76
d	Mudstone	0.490 x 0.365 0.6	11.73	0.013	0.024
e	Siltstone	0.40 x 0.30 1.0	14	NA	13
f	Siltstone	0.140 x 0.120 0.14	20	NA	5.4
g	Carbonate rock	1.20 x 0.90 1.33	17	NA	11.53
h	Carbonate rock	0.25 x 0.20 0.28	20	NA	0.42

The sample image sizes are listed in Table 1 and reconstructions are presented in Figure 1. Multi-scale reconstruction is illustrated via samples e-h. Sample e is a micron scale siltstone image, and sample f is a submicron siltstone image, while sample g is a micron scale carbonate image, and sample h is a submicron carbonate image. For each of these samples only one thin section was available and we assumed that the sections were statistically the same in the remaining perpendicular directions. Visually, the agreement between the sections and the PAMs is good (Fig. 1). However, more detailed comparisons between the images and the reconstructions will be carried out in Sections 3.5 and 4. Comparison of the sections and the PAM shows, for example, that the morphology and size of the void spaces have been qualitatively reproduced.

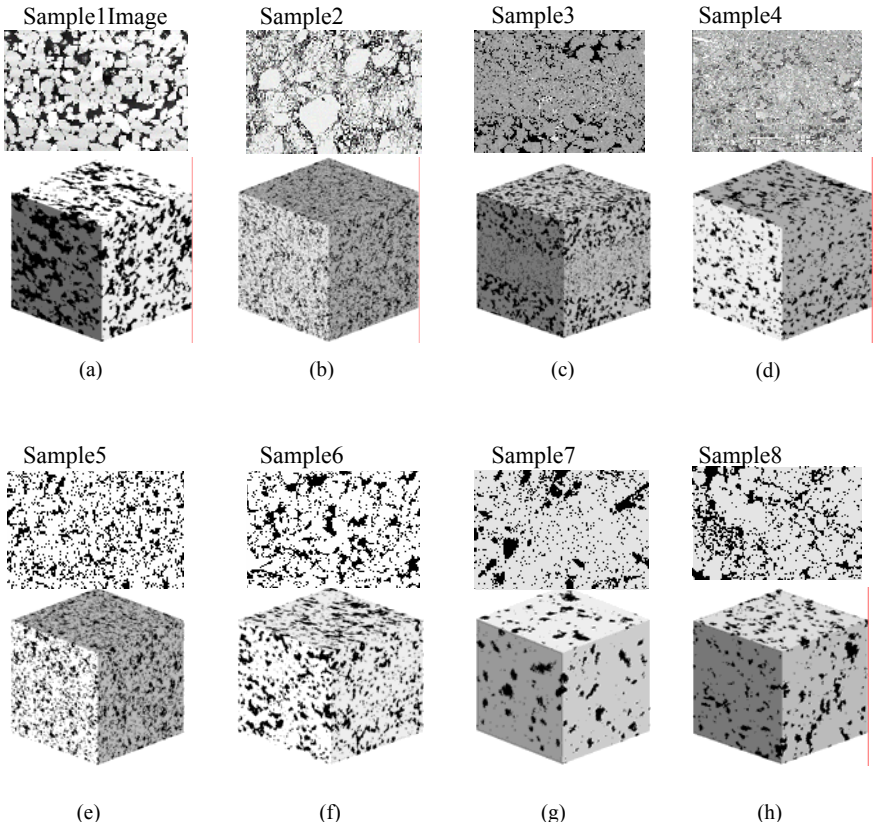

Figure 1. Simulations of various rocks with the corresponding thin sections, for samples a to h as detailed in Table 1 (black indicates pore space).

3. PORE SYSTEM CHARACTERISATION

When a 3D model of the medium (e.g. a 3D tomographic reconstruction, or a PAM) exists, it is necessary to extract the geometry of the pore system using one of several published methods (e.g. Øren *et al.*, 2002; Liang *et al.*, 2000; Silin *et al.*, 2003; Lindquist 2000). In the work reported here, we use an approach that is described in Jiang *et al*. (2007). In brief, the determination of pore-system characteristics can take one of two approaches: one seeks to fit pore elements (typically spheres or balls) into the pore-space model, keeping track of

sizes, positions, and then constructing the connectivity. The other seeks to extract a backbone or network that follows the connections, with pore bodies added to that network. The "ball-fitting" idea is the basis for the method that we use below. Our non overlapping method to partition the pore space into sphere-equivalent components overcomes most of the shortcomings discussed above. In addition, many pore-scale geometrical and topological properties can be easily calculated based on this partitioning, such as pore size distribution, coordination number and Euler characteristic. We have also developed an improved scheme based on the combination of "ball-fitting" and "backbone" approach, which is described in Jiang *et al* (submitted).

Although we will not describe all details of the ball-fitting method, it is worth reviewing a few key concepts that highlight why it is not trivial to characterise the pore system. Due to the complex microstructure and irregular void space shapes within porous medium, an accurate definition of a "pore" is difficult. Dullien (1992) presented the concept of "pore neck" based on the minima in the mean radius of curvature (or hydraulic radius). Further work along similar lines to determine pore space characteristics has been carried out by subsequent workers (Kwiecien 1990, Zhao *et al* 1993). Zhao *et al* (1993) pointed out that many pore necks will be missed when using this approach, while other regions can be mislabelled as necks unless the search for narrowing in the sections is performed in a sufficient number of orientations with respect to the image data set. Callaghan (1991) pointed out that other methods associated with particular geometrical models also had some serious limitations. In our work, we have adapted a widely used sphere-fitting (or ball fitting) method and combined it with a non-overlapping restriction. The general idea of this algorithm is to fit and extract each pore from the pore space in descending order of pore radius before handling any other smaller pores.

3.1 Pore-size quantification using sphere-fitting method

To measure pore sizes equivalent to the maximum ball size, template spheres are required, as illustrated in Figure 2. In our fitting algorithm, pores are extracted step by step from the corresponding 3D image of the porous medium such that the larger pores are extracted before the smaller ones. Based on the relationship between porosity and pore size (Mulder, 1996), the largest possible pore radius can be estimated using the expression:

$$M_r = \left(\frac{3\nu\phi}{4\pi} \right)^{\frac{1}{3}} \tag{2}$$

where M_r is the upper-limit radius of a largest sphere, φ is the porosity and ν the volume of the image. In our algorithm, the sphere of radius M_r is first used in an attempt to fit it into the pore space, then successively smaller template spheres are used, until all pore space are occupied.

(a) (b)

Figure 2 The template discrete spheres. (a), (b): spheres of radius 1, 2 respectively.

When a pore has been identified through the process described above, we use the cubic cutting method to remove it from the pore space to avoid overlapping with pores extracted later in the procedure (Figure 3).

(a) (b) (c)

Figure 3 Pore extraction processes. (a) full fitting with sphere B(p,r-1), (b) 95% fitting sphere B(p,r), (c) correspond to the subsequent cubic cutting

After all pores of size larger than zero have been extracted from the 3D pore space, there exist some remaining voxels that belong to none of the pore bodies (radius≥1) already identified. Our algorithm connects the dead-end smaller pores with larger pores (Fig. 4), and merges boundary voxels with the larger adjacent pore body.

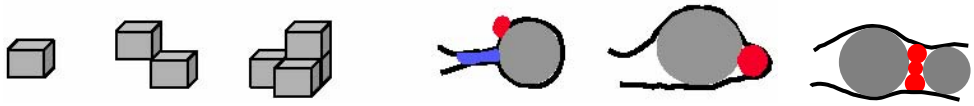

(a) (b) (c) (d) (e) (f)

Figure 4. Merging smaller pores and remaining voxels. (a), (b) and (c) are remaining voxels with radius <1. (d) small pores contribute as pore throat (blue) should be left. (e) Smaller dead end pores (red) which have only one neighbour (grey) of larger size can be merged. (f) Smaller pores (red) next to larger pore can be combined with the larger pore on the left

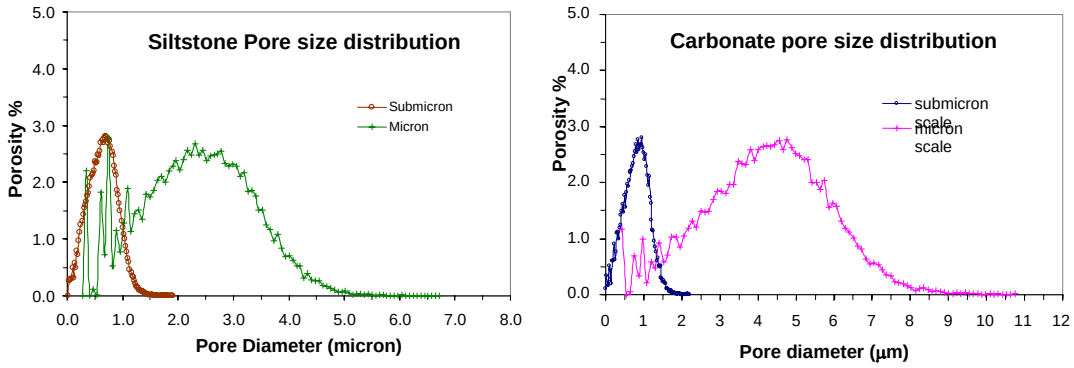

Figure 5. Illustration of pore size distribution curve

As an example, we illustrate the results of the sphere-fitting method by applying it to the two separate scales of both the siltstone and carbonate samples. The resulting pore-size distributions clearly show the effects associated with image resolution (Fig. 5). The higher-resolution models (submicron scale PAM) indicate an average pore-size diameter of approximately 0.6μm in siltstone and 0.8 μm in carbonate. In contrast, the coarse-resolution models (micron scale PAM) show a much larger mode for the pore sizes,

in which the siltstone has an average pore-size diameter of about 2.5 μm and the carbonate has a pore-size of about 4.5 μm. Using a low-order neighbourhood scheme, it is not possible to reproduce all scales simultaneously in the reconstruction. However, it may be possible (see below) to combine the different-scale models to derive a better understanding of the composite material.

3.2 Simulation of mercury injection

The pore geometry and topology data are now available to allow the simulation of mercury intrusion. The mercury injection curve can be used as a guide of pore network linking bond size. Ambegoakar *et al* (1971) used percolation theory to show that the "percolation radius" was associated with the average flow in the network. This radius is where, inserting bonds randomly in the network from the largest down, the network flow "switches on" or starts to conduct globally. This quantity is derived from MICP experiments and Katz and Thomson (1986; 1987) showed that an excellent correlation between the mercury breakthrough radius and the absolute permeability of various rock samples could be obtained. This early literature is applied to single and two-phase flow in O'Carroll and Sorbie (1993). Knackstedt *et al* (1998) reveal that the simulated capillary pressure curves correlated to the heterogeneity even in Berea sandstone. The mercury injection capillary pressure (MICP) curve is calculated using the usual invasion percolation algorithm; the calculated and experimental curves are shown in Fig. 6.

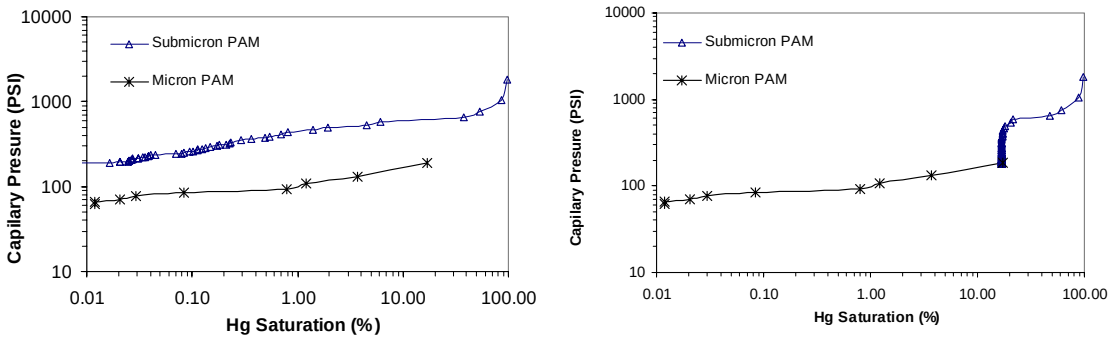

(a) (b)

Figure 6. The calculated MICP curve from the invasion percolation simulator, the mercury injection curves are from two scaled siltstone reconstructions, (a) two mercury curves are drawn in s separate volumetric accumulation, (b) the lower scale (submicron) MICP curve rescaled to continue with the higher scale invasion percolation simulator.

Again, the MICP curve shows that the different pore size structures have distinctive percolation features. It is obvious that the micron scale siltstone has very low capillary pressure, which indicates larger pore sizes. The short length of the curve indicates poor connectivity due to loss of the connecting pore throats below the resolution limit. In contrast, the higher resolution reconstructed PAM has higher capillary pressure because most small pores can be reproduced at this scale and the breakthrough curve is complete in this case. It is interesting to note that the end point capillary pressure in the lower scale

MICP curve coincides with the beginning capillary pressure of the higher scale curve, which suggests that the complete MICP curve can be found by combing the two curves.

4. SUMMARY AND CONCLUSIONS

In this work, we describe an approach for reconstructing and quantifying the pore geometry and topology of porous media. We take as our starting point, 3D rock voxel images which are either generated experimentally by micro-tomography or by a pore reconstruction method (e.g. the PAM approach). We then apply our pore analysis tools (PATs) which are a suite of algorithms which allow us to extract quantified descriptions from which we can build network models for simulating two- and three-phase fluid flow at the pore scale. Indeed, the central purpose of this paper is to present and discuss these detailed algorithms for the pore reconstruction, geometry and topology mapping and quantification. The non-overlapping sphere-fitting method is a simple and efficient approach for quantifying the geometry and topology of 3D reconstructions of porous media. Here, we have applied that method to investigate the multi-scale pore systems of a siltstone and a carbonate. The different scale input images lead to reconstructions that have distinct pore size distributions. The flow behaviour of the resulting models (here illustrated via simulated mercury injection curves) is quite different, as would be expected from materials with those contrasting characteristics. The separate mercury injection curves seem to represent distinct pore systems in the samples. Those pore systems will, in the real sample, interact. Our combined mercury injection curve represents a naive but plausible prediction of the bulk flow characteristics of this sample. Further work is necessary to investigate a range of ways of combining multi-scale models to attain better estimates of bulk flow properties. Nevertheless, the results presented here suggest that there is reason to expect that such multi-scale materials can be successfully characterised by separate analysis of the properties of their component parts.

Acknowledgement

The authors acknowledge funding from EPSRC under grant number EP/D002435/1.

REFERENCES

Ambegaokar, V., Halperin, B.I., and Langer, J.S., *Phys. Rev*. B, 4 , p.2612, 1971.

Arns, C.H. , Knackstedt, M.A., Pinczewski, W.V. and Lindquist, W.B. "Accurate computation of transport properties from microtomographic images". *Geophys. Res. Lett.* **28** (2001), pp. 3361–3364.

Bakke, S., Øren, P.E., 1997. 3-D pore-scale modeling of sandstone and flow simulations in pore networks. *SPE J.*, **2,** 136.

Biswal, B., Manwarth, C., Hilfer, R., 1998. Three-dimensional local porosity analysis of porous media. *Physica*. A **255**, 221–241.

Biswal, B., Manwart, C., Hilfer, R., Bakke, S., Øren, P.E., 1999. Quantitative analysis of experimental and synthetic microstructure for sedimentary rock. *Physica A*, **273**, 452-475.

Blunt, M., Zhou, D., Fenwick, D., 1995. Three-phase flow and gravity drainage in porous media. *Transport in Porous Media* **20**, 77– 103.

Callaghan, P. T., ''Principles of Nuclear Magnetic Resonance Microscopy.'' Clarendon, Oxford, 1991.

Dunsmoir, J.H., Ferguson, S.R., D'Amico, K.L., Stokes, J.P., 1991. X-ray microtomography: a new tool for the characterization of porous media. *Proceedings of the 1991 SPE Annual Technical Conference and Exhibition*, Dallas, Oct. 6 – 9.

Fatt, I., 1956. The network model of porous media: I. Capillary pressure characteristics. *Trans*. *AIME* **207**, 114.

Hazlett, R.D., 1997. Statistical characterization and stochastic modeling of pore networks in relation to fluid flow. *Mathematical Geology* **29**, 801–822.

Hazlett, R.D., Chen, S.Y., Soll, W.E., 1998. Wettability and rate effects on immiscible displacement: Lattice Boltzmann simulation in microtomographic images of reservoir rocks. *Journal of Petroleum Science and Engineering* **20**, 167–175.

Jiang, Z., Wu, K., Couples, G.D., van Dijke, M.I.J. and Sorbie, K.S. 2007. "Efficient extraction of networks from 3d porous media". Accepted by *Water Resources Research*

Joshi, M., 1974. A class of stochastic models for porous media. PhD thesis, University of Kansas.

Katz, A.J. and Thompson, A.H. , *Phys. Rev.* B, **34**, p. 8179, 1986.

Knackstedt, M.A., Sheppard, A. P., and Pinczewski, W. V. 1998. "Simulation of mercury porosimetry on correlated grids: Evidence for extended correlated heterogeneity at the pore scale in rocks", Physical Review E **58**, R6923

Kwiecien, M. J., Macdonald, I. F., and Dullien, F. A. L., *J. Microsc.* **159,** 343, 1990.

Lindquist, W.B., Venkatarangan, A., Dunsmuir, J., and Wong, T. F., Pore and throat size distributions measured from synchrotron x-ray tomographic images of Fontainbleau sandstones: *J. Geophys. Res*., **105B**, 21508, 2000.

Mani, V., Mohanty, K.K., 1998. Pore-level network modelling of three-phase capillary pressure and relative permeability curves. *SPE Journal* **3**, 238– 248.

Manswart, C., Hilfer, R., 1998. Reconstruction of random media using Monte Carlo methods. *Physical Review*. E **59**, 5596– 5599.

Manswart, C., Torquato, S., Hilfer, R., 2000. Stochastic reconstruction of sandstones. *Physical Review*. E **62**, 893–899.

O'Carroll, C. and Sorbie, K.S., "Generalisation of the Poiseuille Law for One and Two Phase Flow in a Random Capillary Network", *Phys. Rev.* E, **47** (No. 5), pp. 3467 – 3476, 1993.

Okabe, H., and Blunt, J. M., 2004. "Prediction of permeability for porous media reconstructed using multiple-point statistics", *PHYSICAL REVIEW* E **70**, 066135 (2004)

Øren, P.E., Pinczewski, W.V., 1992. Mobilization of waterflood residual oil by gas injection for water wet systems. *SPE Formation Evaluation* **7**, 70–78.

Øren, P.E., Bakke, S., 2002. Process based reconstruction of sandstones and predictions of transport properties. *Transport in Porous Media* **46**, 311– 343.

Quiblier, J.A., 1984. A new three-dimensional modelling technique for studying porous media. *Journal of Colloid and Interface Science* **98**, 84– 102.

Roberts, A.P., 1997. Statistical reconstruction of three-dimensional porous media from two dimensional images. *Physical Review*. E **56**, 3203– 3212.

Silin, D, B. and Patzek, T. W., Robust determination of the pore space morphology in sedimentary rocks , *Soc. Petrol. Eng. J.,* 84296, 2003.

Spanne, P., Thovert, J. F., Jacquin, C. J., Lindquist, W. B., Jones, K. W., and Adler, P. M., *Phys. Rev. Lett.* **73**, 2001, 1994.

van Dijke, M.I.J. and Sorbie, K.S., 2002. Pore-scale network model for three-phase flow in mixed-wet porous media. *Physical Review*. E **66**, 046302.

Wu, K., van Dijke, M.I.J. Couples, G.D., Jiang, Z., Ma, J., and Sorbie, K.S. 2006. "**A** New 3D Stochastic Model to Characterise Heterogeneous Porous Media, Applications to Reservoir Rocks". *Transport in Porous Media* **65**, 443-467.

Yeong, C.L.Y., Torquato, S., 1998. Reconstructing random media. *Physical Review.* E **57**, 495– 506

Zhao, H. Q., and Macdonald, I. F., *J. Microsc.* **172**, 157, 1993.